Pavlo HERASYMENKO

Institute of Electrodynamics of the National Academy of Sciences of Ukraine

doi:10.15199/48.2021.03.13

Mathematical analysis of dual-frequency load current of two-inverter power supply for induction heating systems

Abstract. *The aim of this research work is to obtain analytical expressions that allow analyzing the dual-frequency current of the induction coil, as well as, the currents of the inverters for the "two inverter power supplies" converter topology. To take into account frequency-dependent parameters of an induction heater load, their implementation is shown through series-parallel connections of frequency-independent resistances and inductances. A simulation study is performed to verify the obtained analytical expressions of the currents.*

Streszczenie. *Celem artykułu było otrzymanie analitycznego opisu umożliwiającego analizę prądu podwójnej częstotliwości stosowanego w nagrzewaniu indukcyjnym. Analizowano prąd w cewce oraz współpracującego z nią przekształtnika. Przeprowadzono też symulację potwierdzającą model analityczny. (**Analiza matematyczna dwuczęstotliwościowego systemu nagrzewania indukcyjnego**)*

Keywords: dual-frequency converter, induction heating, mathematical analysis, resonant inverter, simulation.
Słowa kluczowe: nagrzewanie indukcyjne, system dwuczęstotliwościowy, przekształtniki.

Introduction

Induction heating (IH) provides contactless, energy efficient, accurate and fast heating of electrically conductive materials. Due to its advantages, IH is increasingly used in different fields such as industry, medicine and the household sector [1]. One of the technological tasks for which IH is used in the industrial manufacturing sector is surface hardening. Some parts of non-uniform cylindrical shapes, such as splined hubs, sprockets, and gears, require a special heat treatment process to obtain a uniform hardened pattern by using circular inductors. For shapes of such parts, it is impossible to achieve the required pattern with only one frequency. The best results are obtained with dual and triple frequency approach. Thus, in recent years, many converters' topologies that can provide dual-frequency output current have been proposed. Often, while designing a converter, it is necessary to make a lot of practical experiments to optimize commutation modes of converter transistors, to determine the transformation ratio of a converter matching transformer, etc. Modelling is an important step after the analysis of real systems. Mathematical analysis with computer modelling and simulation help to avoid a big number of experiments and provide a better understanding of the process in a converter. Therefore, for the efficient design of converters, it is necessary to have models that correctly describe such converters and their loads.

The key parameters of IH are the current frequency and the duration of heating. They allow controlling temperature distribution which must be adjusted to a contour of hardness, to be finally obtained. Gear hardening processes have been conducted for many years [2-6]. However, although the IH process is well described in the scientific literature and is used in many industry technologies, its application for the hardening of gear wheels is still rather rare. In the case of gear wheels, hardening should occur on a surface, including the side surface, and the top and root of a workpiece tooth. It is very difficult to generate equally distributed eddy currents on the surface of the workpiece with a single-frequency inverter. The solution is to use a dual-frequency converter. The load current i_L, flowing through the induction coil, consists of two components: medium frequency (MF) current i_{MF} and high frequency (HF) current i_{HF}. HFs are required to heat the surfaces nearer to the induction coil (the top and flanges of the teeth), and MFs heat the quasi-cylindrical area near the surface of the part (the root area of the teeth) (Fig. 1). Properly matched frequencies and amplitudes (i_{MF} and i_{HF}) allow reaching even heat surface distribution.

Fig.1. Example of single- and dual-frequency inverters application area

The need for dual-frequency current in the induction coil has led to the emergence of different converters' topologies and to researches its control methods.

In [7-9] is proposed a quasi-resonant inverter with two resonant capacitors. However, this circuit cannot produce HF and MF currents simultaneously, that is, the hardening of parts takes place through two successive heating processes. For example, surface hardening process takes place in two successive steps. Also, the operating frequency range of this inverter is not wide. The authors of [10] have proposed inverter topology with one resonant capacitor and a two-way short circuit switch across the capacitor. In this topology, the output frequency is controlled by regulation the duration of an on/off-interval of the two-way switch, simultaneous application HF and MF currents is impossible. To ensure dual-frequency current simultaneously, in [11] by the same authors have been proposed inverter topology with two capacitors and a polarity providing circuit. Such topology has a large number of switching devices and the frequencies of the currents MF and HF are connected. The inverter topology with pulse-width modulation for dual-frequency current simultaneously has been presented in [12] and [13]. The dual-frequency current is obtained by a single inverter. HF wave is modulated by the MF wave to produce dual-frequency output. Output control is achieved by variation of the amplitude of MF wave and frequency of HF wave. The main disadvantage of such inverter topology is related to hard commutation modes of the inverter's transistors. Multilevel inverter configuration for dual-frequency output is proposed in [14]. The authors of [14] have proposed and analyzed multilevel inverter with both equal and unequal sources for this application. However, such configuration needs independent power supplies. In [15], is presented the topology of a converter based on two single-frequency series-resonant inverters, each of which works

independently to its own frequency range. The amplitudes of both frequencies are independently controllable, which allows separate regulation of the respective shares of the output power of both frequencies, according to the requirements of the workpiece. Power regulation can be achieved by using different control techniques [16-19].

This paper presents the mathematical analysis of the dual-frequency load current of a transistor converter for induction heating systems. The converter is based on a two single-frequency voltage-source series-resonant inverter configuration. There is shown implementation frequency-dependent parameters of an induction heater load through series-parallel connections of frequency-independent resistances and inductances in the paper. The presented an obtained as a result of the analytical solution the analytical expressions of the currents allow modeling the currents under different load parameters and values of the series-resonant circuits of the inverters. The schematic model of the converter has been developed using the blocks in the MATLAB/Simulink graphical interface. Comparing the calculated result of the current with the simulation results shows a deviation no more than 10.04% for the load current.

Basic of induction heating

Fig. 2 shows a very basic system, consisting of the induction heating coil with a workpiece and AC voltage source, to explain electromagnetic induction and skin effect. The most basic elements composing an IH system are the piece to be heated, also known as the workpiece, and the induction coil or inductor that produces the magnetic field needed to generate the heat. The power supply generates AC voltage, with necessary frequency and amplitude, that it supplies to the induction coil. The induction coil and the workpiece may have any shape and the workpiece is usually placed inside a circular coil to achieve a better coupling [20]. The typical operating frequencies of these systems range from line frequency as far as a few MHz [1].

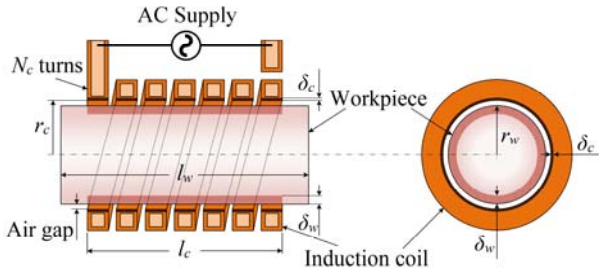

Fig.2. Basic system: induction heating coil – AC voltage source

IH phenomenon relies on two mechanisms of energy dissipation: Energy losses due to Joule effect and Energy losses due to hysteresis. [1, 21-23]. The basic nature of induction heating is that the eddy currents are produced on the outside of the workpiece in what is often referred as "skin effect" heating. The density of the induced current diminishes when flowing closer to the center [23-24].

In the case of flat thick bodies with constant electromagnetic properties, the penetration depth or skin depth δ is defined as the thickness of the surface layer at which only 63% of current flows and approximately 86% of heat is generated due to current resistance [21, 22, 24]. The penetration depth, depending on the frequency and the two properties of the material (resistivity and relative permeability), is defined as:

$$\delta = \sqrt{\frac{\rho}{\pi \mu_0 \mu_r f}} \text{ , [m]} \tag{1}$$

where: ρ is the electrical resistivity of the material [Ω·m], μ_0 is the magnetic permeability of free space ($4\pi \times 10^{-7}$ [H/m]), μ_r is the relative permeability of the workpiece material, f is the supply frequency [Hz].

Modeling equivalent parameters of induction heating coil with workpiece

There are many analytical methods for determining the equivalent circuit parameters of the induction coil–workpiece system [25-26]. Given the need for a precise, but a simple model of an induction heater load (induction coil–workpiece), Baker's method was often used [25]. Baker's method of calculation of the equivalent circuit parameters was based on the equations for the infinitely long coil and workpiece.

The induction coil and workpiece can be modelled as a series equivalent circuit (SEC), which consists of a serial connection of inductances and resistances [22, 26]. In the case of using short induction coils (which is typical for surface hardening non-uniform cylindrical parts by the dual-frequency current), the induction coil and workpiece can be modelled as with a transformer equivalent circuit (TEC) model [26].

If the leads of the induction coil have a complicated shape, the resistance and reactance can be defined as the sum of the resistances and reactances of the equivalent rectangular sections of this lead.

In case of the SEC model, all components (resistors and reactances) are in series, so the induction coil and the workpiece can be easily represented by an equivalent series circuit: an equivalent resistance R_{EQ} and equivalent inductance L_{EQ} are connected in series. The TEC is a little harder than the SEC, but it can be also replaced by a series connection of R_{EQ} and L_{EQ}.

In both cases, the total series impedance is

$$Z = R_{EQ} + jX_{EQ} = R_{EQ} + j2\pi f L_{EQ} \, . \tag{2}$$

The values of R_{EQ} and L_{EQ} are frequency dependent. Therefore, in modelling the frequency dependence of these parameters can be used the width band frequency model (the equivalent circuit with constant parameters) (Fig. 3). [27-29].

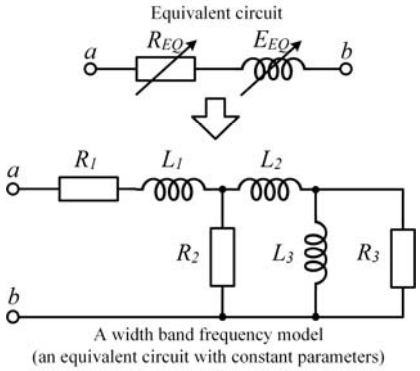

Fig.3. Width band frequency model of equivalent load circuit

In this case, the equivalent resistance and inductance of the scheme in Fig. 3 are defined as

$$R_{EQ}(f) = R_2 + R_1 - R_2^2 \times \frac{R_2 R_3^2 + (2\pi f)^2 L_3^2 (R_2 + R_3)}{\left(R_2 R_3 - (2\pi f)^2 L_2 L_3\right)^2 + (2\pi f)^2 \left(L_3 R_3 + L_2 R_3 + L_3 R_2\right)^2} \, , \tag{3}$$

$$L_{EQ}(f) = L_1 + R_2^2 \times \tag{4}$$

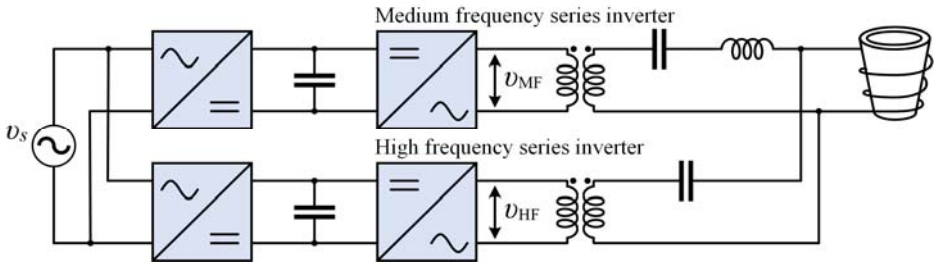

Fig.4. “Two inverter power supplies” converter topology

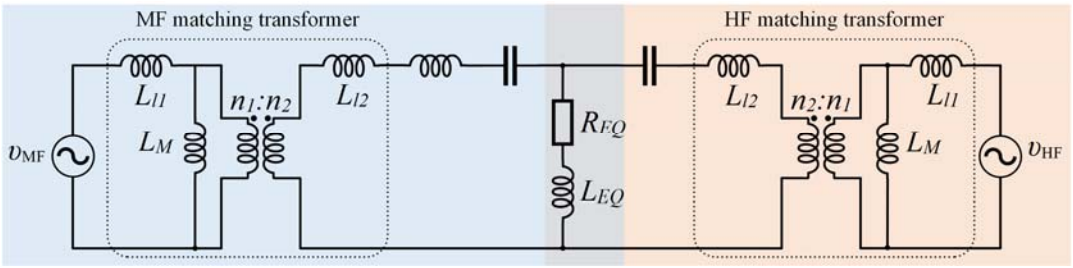

Fig.5. Simplified equivalent circuit of system “AC voltage sources – induction heating coil with workpiece”

$$\frac{(2\pi f)^2 L_2 L_3^2 + R_3^2 (L_2 + L_3)}{\left(R_2 R_3 - (2\pi f)^2 L_2 L_3\right)^2 + (2\pi f)^2 (L_3 R_3 + L_2 R_3 + L_3 R_2)^2}.$$

Parasitic connection circuit parameters between the matching transformer and the induction coil can be integrated into R_1 and L_1.

Topology of “two inverter power supplies”

Fig. 4 depicts the structure of the power supply where MF and HF are generated separately, by using two voltage-source series-resonant inverters, two frequency resonant circuits of which connect the output of the inverters to the induction coil.

Fig. 5 shows a simplified equivalent circuit of the system “AC voltage sources – induction heating coil with workpiece” in which the matching transformers of the MF and HF inverters are presented through the T-model of a transformer, and the output voltages of the inverters are represented as voltage sources. The presented T-models of the matching transformers on Fig. 5 contain the magnetizing (L_M) and leakage (L_{l1}, L_{l2}) inductances, as well as the ideal transformers with some turns ratios n_1:n_2. L_{l1} and L_{l2} are the primary and secondary sides leakage inductances of the transformers, respectively, and n_1 and n_2 are the turns numbers of the primary and secondary windings of the transformers, respectively.

Due to the fact that the values of the magnetizing inductances of T-models are much bigger than the values of the leakage inductances, their influence can be neglected. In this case, the equivalent circuit in Fig. 5 can be represented as it is shown in Fig. 6. In Fig. 6 C_{MF} and C_{HF} are the capacitors of the resonant circuits of the MF and HF inverters, respectively. The inductance L_{MF} represents the sum of the inductance of the resonant circuits of the MF inverter (not including L_{EQ}), the inductance L_{l2} and the reflected to the secondary side of the MF matching transformer the inductance L_{l1}. The inductance L_{HF} represents the sum of the inductance L_{l2} and reflected to the secondary side of the HF matching transformer the inductance L_{l1}. The voltage sources v'_{MF} and v'_{HF} are the equivalent voltage sources of v_{MF} and v_{HF}, which are reflected to the secondary side of the matching transformers.

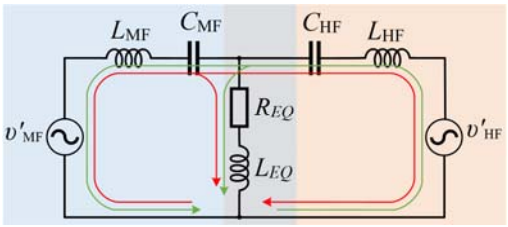

Fig.6. Represented simplified equivalent circuit of system “AC voltage sources – induction heating coil with workpiece”

a)

b)

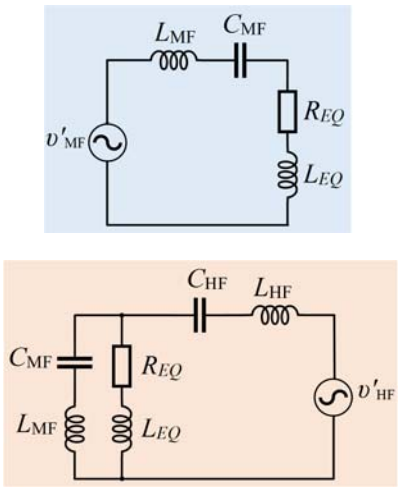

Fig.7. Equivalent circuits

The capacitor C_{HF} provides a waveform of the HF inverter output current almost sinusoidal and also serves as a filter to block the low-frequency component of the load current, which is due to the LF inverter. Thus, the influence of source v'_{MF} on the current in the circuit of the source v'_{HF} can be negated. In this case, an equivalent circuit of the system “v'_{MF} source – induction heating coil with workpiece” is of the form as it is shown in Fig. 7,a. In the case of the

influence of source υ'_{HF} on the current in the circuit of the source υ'_{MF}, the value of L_{MF} could be insufficient to negate the influence of source υ'_{HF}. In this case, an equivalent circuit of the system "υ'_{HF} source – induction heating coil with workpiece" is of the form as it is shown in Fig. 7,b.

For presented circuits on Fig. 7, the total series impedance connected to υ'_{MF} is given by

(5) $$Z_{\mathrm{MF}} = \sqrt{R_{EQ}\left(f_{\mathrm{MF}}\right)^2 + \left(2\pi f_{\mathrm{MF}}\left(L_{\mathrm{MF}} + L_{EQ}\left(f_{\mathrm{MF}}\right)\right) - \frac{1}{2\pi f_{\mathrm{MF}} C_{\mathrm{MF}}}\right)^2}.$$

and the total series impedance connected to υ'_{HF} is given by

(6) $$Z_{\mathrm{HF}} = \sqrt{R_{\mathrm{HF}}^2 + X_{\mathrm{HF}}^2}$$

where

(7) $$R_{\mathrm{HF}} = R_{EQ}\left(f_{\mathrm{HF}}\right)\frac{\left(2\pi f_{\mathrm{HF}} L_{\mathrm{MF}} - \frac{1}{2\pi f_{\mathrm{HF}} C_{\mathrm{MF}}}\right)^2}{\left(2\pi f_{\mathrm{HF}}\left(L_{\mathrm{MF}} + L_{EQ}\left(f_{\mathrm{HF}}\right)\right) - \frac{1}{2\pi f_{\mathrm{HF}} C_{\mathrm{MF}}}\right)^2 + R_{EQ}\left(f_{\mathrm{HF}}\right)^2}$$

(8) $$X_{HF} = \left(\frac{1}{2\pi f_{\mathrm{HF}} C_{\mathrm{MF}}} - 2\pi f_{\mathrm{HF}} L_{\mathrm{MF}}\right) \times \frac{\left(\frac{L_{EQ}\left(f_{\mathrm{HF}}\right)}{C_{\mathrm{MF}}} - \left(2\pi f_{\mathrm{HF}}\right)^2 L_{EQ}\left(f_{\mathrm{HF}}\right)\left(L_{\mathrm{MF}} + L_{EQ}\left(f_{\mathrm{HF}}\right)\right)\right) - R_{EQ}\left(f_{\mathrm{HF}}\right)^2}{\left(2\pi f_{\mathrm{HF}}\left(L_{\mathrm{MF}} + L_{EQ}\left(f_{\mathrm{HF}}\right)\right) - \frac{1}{2\pi f_{\mathrm{HF}} C_{\mathrm{MF}}}\right)^2 + R_{EQ}\left(f_{\mathrm{HF}}\right)^2} + 2\pi f_{\mathrm{HF}} L_{\mathrm{HF}} - \frac{1}{2\pi f_{\mathrm{HF}} C_{\mathrm{HF}}}$$

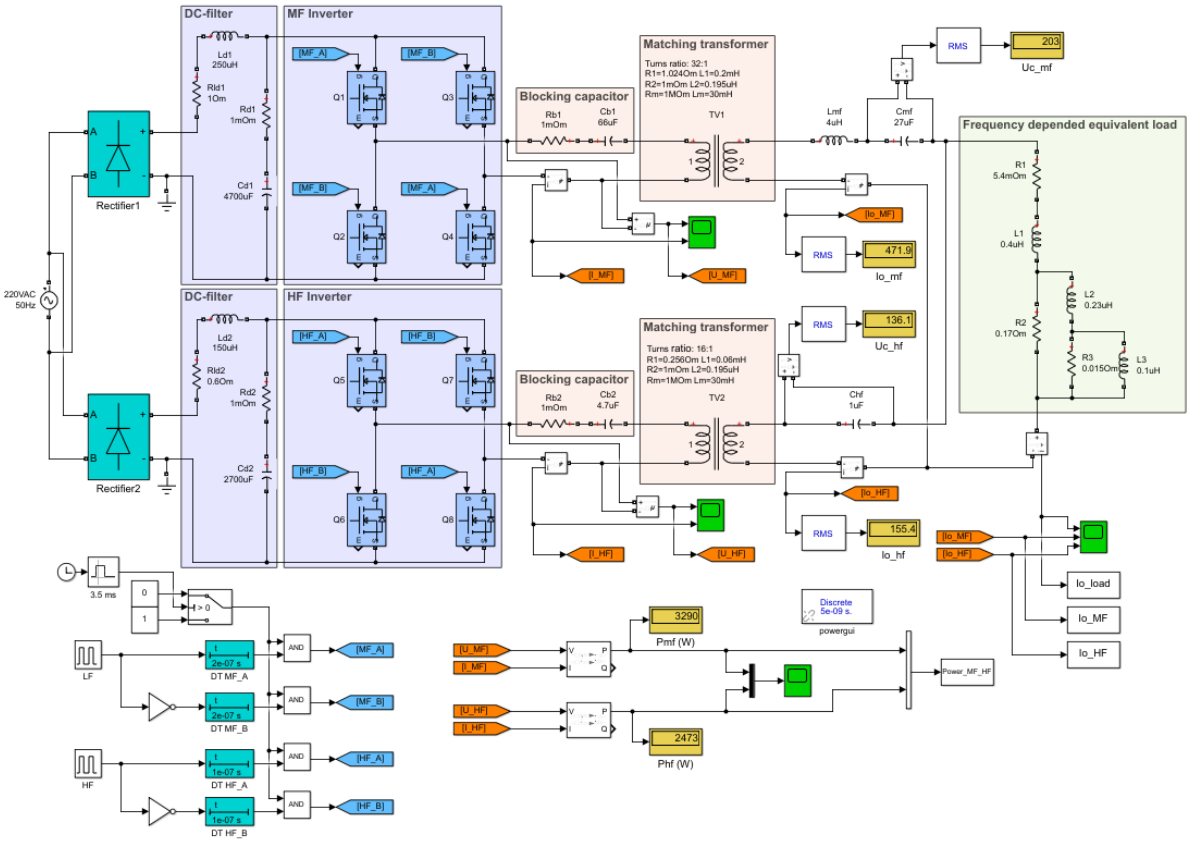

Fig.8. Transistor converter of the topology of "two inverter power supplies" in MATLAB/Simulink environment.

The currents of υ'_{MF} and υ'_{HF} are given by

(9) $$i_{\mathrm{HF}} = \frac{\upsilon'_{\mathrm{HF}}}{Z_{\mathrm{HF}}},$$

(10) $$i_{\mathrm{MF}} = \frac{\upsilon'_{\mathrm{MF}}}{Z_{\mathrm{MF}}} - \left(\frac{\upsilon'_{\mathrm{HF}} - i_{\mathrm{HF}}\left(2\pi f_{\mathrm{HF}} L_{\mathrm{HF}} - \frac{1}{2\pi f_{\mathrm{HF}} C_{\mathrm{HF}}}\right)}{\left(2\pi f_{\mathrm{HF}} L_{\mathrm{MF}} - \frac{1}{2\pi f_{\mathrm{HF}} C_{\mathrm{MF}}}\right)}\right),$$

and the equivalent load current is given by

(11) $$i_L = \frac{\upsilon'_{\mathrm{MF}}}{Z_{\mathrm{MF}}} + \left(\frac{\upsilon'_{\mathrm{HF}} - i_{\mathrm{HF}}\left(2\pi f L_{\mathrm{HF}} - \frac{1}{2\pi f C_{\mathrm{HF}}}\right)}{\sqrt{R_{EQ}^2 + \left(2\pi f L_{EQ}\right)^2}}\right).$$

Simulation and calculation results

In order to investigate the validity of the equations obtained by the mathematical analysis in this paper, the transistor converter of the topology of "two inverter power supplies" has been simulated in MATLAB/Simulink environment (Fig. 8). The converter contains two single-frequency inverters, operating frequencies which are set by two independent generators. Two matching transformers are used to match the equivalent load impedance with the output voltage of each inverter. The load is modelled by the width band frequency model.

In order to determine R_{EQ} and L_{EQ}, a short induction coil (Fig. 9) was developed and experimental measurement of R_{EQ} and L_{EQ} values were carried out with precision LCR meter BR2876-5 (basic accuracy in 0.05% for R, L, and C measurement). Based on the measured values of R_{EQ} and L_{EQ}, the values of the elements of the width band frequency model was determined (Fig. 8 – "frequency depended equivalent load").

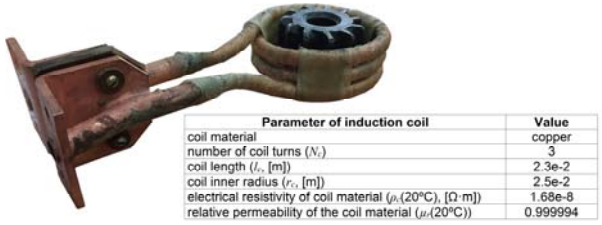

Parameter of induction coil	Value
coil material	copper
number of coil turns (N_c)	3
coil length (l_c, [m])	2.3e-2
coil inner radius (r_{in}, [m])	2.5e-2
electrical resistivity of coil material (ρ_c(20°C), [Ω·m])	1.68e-8
relative permeability of the coil material (μ_{rc}(20°C))	0.999994

Fig.9. Developed short induction coil.

The plotted results in Fig. 10 demonstrate the obtained waveforms of the load current and MF and HF currents on the secondary sides of the matching transformers obtained as the simulation and calculation results. For calculation the sources v'_{MF} and v'_{HF} were represented by sinusoidal sources, amplitudes of which are equal to the first harmonics of v'_{MF} and v'_{HF}, respectively.

The accuracy of the obtained analytical expressions of the currents i_{MF}, i_{HF} and i_L was verified by comparing of the calculated values of the currents using (9)-(11) with the value obtained as a result of simulation:

$$\Delta = \frac{\left| I_{CAL} - I_{SIM} \right|}{I_{SIM}} \times 100\% , \tag{12}$$

where: I_{CAL} is the calculated current value determined from (9)-(11) and I_{SIM} is the current value obtained as a result of the simulation

The maximal deviation Δ between the calculated and simulated values of the currents is: 0.21% for i_{MF}, 4.47% for i_{HF}, and 10.04% for i_L. The deviation of 10.04% for i_L can be explained by the fact that capacitor C_{HF} cannot completely filter out the influence of the source v'_{MF} on the source v'_{HF}. Therefore, if it is necessary to obtain higher accuracy in determining i_L, the equivalent circuit of the system "v'_{MF} source – induction heating coil with workpiece" (Fig. 7,a) must be corrected and corresponding changes have to be made to the analytical expressions. Furthermore, albeit to a lesser extent, the deviation is influenced by the fact that the output voltages of the MF and HF inverters are represented through the first harmonics.

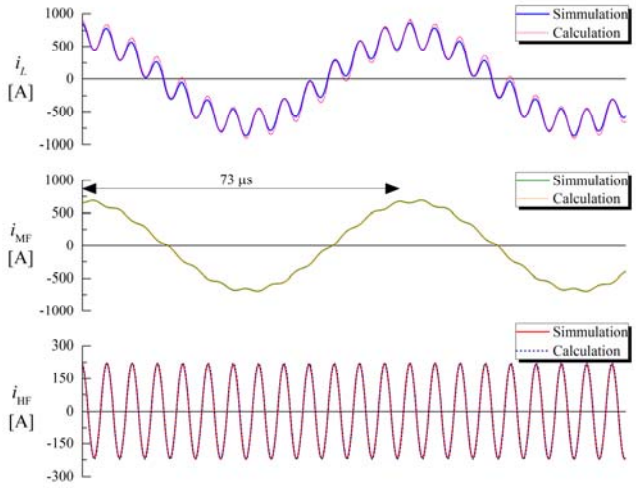

Fig.10. Waveforms of load current and MF and HF currents on secondary sides of matching transformers obtained as simulation and calculation results.

Conclusion

This paper has discussed the mathematical analysis of the dual-frequency load current of the two-inverter power supply for induction heating systems. The obtained analytical expressions of the load current and MF and HF currents of the series-resonant circuits of the two-inverter power supply allow modeling the currents under different load parameters and values of the series-resonant circuits of the inverters. Comparing of the calculated result of the current with the simulation results shows a deviation no more than 10.04% for the load current.

***Authors**: PhD Pavlo Herasymenko, Senior Researcher of Department of Transistor Converters, Institute of Electrodynamics of the National Academy of Sciences of Ukraine, 56 Peremohy prosp., office 457, 03680, Kyiv, Ukraine, E-mail: herasymenko@ieee.org.*

REFERENCES

[1] Lucia O., Maussion P., Dede E.J., Burdio J.M., Induction heating technology and its applications: past developments, current technology, and future challenges, *IEEE Transactions on Industrial Electronics*, 61 (2014), No. 5, 2509-2520

[2] Rudnev V., Single-coil dual-frequency induction hardening of gears, *Heat Treating Progress*, 9 (2009), No. 6, 9-11

[3] Schwenk W.R., Simultaneous dual-frequency induction hardening, *Heat Treating Progress*, (2003), 35-38

[4] Przylucki R., Smalcerz A., Induction heating of gears - Pulsing dual-frequency concept, *Metalurgija*, 52 (2013), 235-238

[5] Petzold T., Modelling, analysis and simulation of multifrequency induction hardening, *Dissertation*, Technical University of Berlin, Berlin, Germany, (2014)

[6] Legutko P., Kierepka K., Zimoch P., Simultaneous dual-frequency inverter for induction hardening of gears, *Przeglad Elektrotechniczny*, 94 (2018), No. 12, 74-78 (Polish)
[7] Okudaira S., Nomura K., Matsuse K., New quasi-resonant inverter for induction heating, *Conference Record of the Power Conversion Conference*, (1993), 117-122
[8] Okudaira S., Matsuse K., Power control of an adjustable frequency quasi-resonant inverter for dual frequency induction heating, *Third International Power Electronics and Motion Control Conference*, (2000), 968-973
[9] Okudaira S., Matsuse K., Adjustable frequency quasi-resonant inverter circuits having short-circuit switch across resonant capacitor, *IEEE Transactions on Power Electronics*, 23 (2008), No. 4, 1830-1838
[10] Okudaira S., Matsuse K., A new quasi-resonant inverter with two-way short-circuit switch across a resonant capacitor, *Proceedings of the Power Conversion Conference*, (2002), 1496-1501
[11] Okudaira S, Matsuse K., Dual frequency output quasi-resonant inverter for induction heating, *IEEJ Transactions on Industry Applications*, 121 (2001), No. 5, 563-568
[12] Esteve V., Jordan J., Sanchis-Kilders E., Dede E.J., Maset E., Ejea J.B., Ferreres A., Comparative study of a single inverter bridge for dual-frequency induction heating using Si and SiC MOSFETs, *IEEE Transactions on Industrial Electronics*, 62 (2015), No. 3, 1440-1450
[13] Esteve V., Jordan J., Dede E.J., Sanchis-Kilders E., Maset E., Induction heating inverter with simultaneous dual-frequency output, *Twenty-First Annual IEEE Applied Power Electronics Conference and Exposition*, (2006), 1505-1509
[14] Diong B., Corzine K., Basireddy S., Lu Shuai., Multilevel inverter-based dual-frequency power supply, *IEEE Power Electronics Letters*, (2003), No. 4, 115-119
[15] Schwenk W., Hsussler A., Heiliger A., *European Patent*, EP 1363474 A2 (2003)
[16] Grajales L. and Lee F.C., Control system design and small-signal analysis of a phase-shift-controlled series-resonant inverter for induction heating, *Proceedings of PESC '95 - Power Electronics Specialist Conference*, (1995), 450-456
[17] Nagai S., Michihira M., Nakaoka M., New phase-shifted soft-switching PWM high-frequency series resonant inverters topologies and their practical evaluations, *1994 Fifth International Conference on Power Electronics and Variable-Speed Drives*, (1994), 274-279
[18] Young-Sup Kwon, Sang-Bong Yoo and Dong-Seok Hyun, Half-bridge series resonant inverter for induction heating applications with load-adaptive PFM control strategy, *APEC '99. Fourteenth Annual Applied Power Electronics Conference and Exposition*, (1999), 575-581
[19] Fujita H. and Akagi H., Control and performance of a pulse-density-modulated series-resonant inverter for corona discharge processes, *IEEE Transactions on Industry Applications*, 35 (1999), No. 3, 621-627
[20] Zinn S., Semiatin S.L., Coil design and fabrication. Part1: Basic design and modifications, *Heat treating*, (1988), 32-36
[21] Davies E.J., Conduction and induction heating, The institution of engineering and technology, (1990), 416 pages
[22] Segura G.M., Induction heating converter's design, control and modeling applied to continuous wire, *Doctoral Thesis*, Polytechnic University of Catalonia, Barcelona, Spain, (2012)
[23] AN-9012. Induction Heating System Topology Review. 2013. URL: https://www.onsemi.jp/pub/Collateral/AN-9012.pdf.pdf
[24] Haimbaugh R.E., Practical induction heat treating. Second edition, Ohia: ASM International, (2015), 379 pages
[25] Baker R. M., Design and calculation of induction heating coils, *AIEE Transactions*, 76 (1957), 31-40
[26] Takau L., Improved modelling of induction and transduction heaters, *Doctoral thesis*, University of Canterbury, Christchurch, New Zealand, (2015)
[27] Yen Chu-Sun, Fazarinc Z., Wheeler R.L., Time-domain skin-effect model for transient analysis of lossy transmission lines, *Proceedings of the IEEE*, 70 (1982), No. 7, 750-757
[28] Laboure E., Costa F., Gautier C., Melhem W., Accurate simulation of conducted interferences in isolated DC to DC converters regarding to EMI standards, *27th Annual IEEE Power Electronics Specialists Conference*, (1996), 1973-1978
[29] Forest F., Laboure E., Costa F., Gaspard J.Y., Principle of a multi-load/single converter system for low power induction heating, *IEEE Transactions on Power Electronics*, 15 (2000), No. 2, 223-230